processes

MDPI

Supplementary Materials

Large-Scale Production of Size-Adjusted β-Cell Spheroids in a Fully Controlled Stirred-Tank Reactor

Florian Petry and Denise Salzig *

Institute of Bioprocess Engineering and Pharmaceutical Technology, University of Applied Sciences Mittelhessen, Wiesenstrasse 14, 35390 Giessen, Germany; florian.petry@lse.thm.de

* Correspondence: denise.salzig@lse.thm.de; Tel.: +49-641-309-2630; Fax: +49-641-309-2553

1.1. Theoretical background

As the spheroid formation in a STR is complex, we want to provide more theoretical background for a better understanding of our results. The forces/stress within a STR can be divided into three categories: (a) hydrodynamic stress, resulting from different relative velocities in the culture medium; (b) collision stress, caused by the impact of cells on other cells, or on parts of the bioreactor; and (c) stress, caused by gassing and cell damage due to bubble implosion. Given the similar density of cells and the culture medium [1], and the general low oxygen uptake of mammalian cells, stress induced by collisions and gassing can be ignored at the 1L-scale considered here [2–4]. The hydrodynamic stress can be divided into tensile, compression, and shear forces. Cells exposed to an accelerated flow are subject to tensile forces, whereas those exposed to a decelerated flow are subject to compression forces [5]. Shear forces result from the movement of liquid layers with different relative velocities [1]. As we aim to adjust the spheroid size within our β-cell manufacturing process, we need to reach the above-mentioned steady state when the spheroid strength equals the hydrodynamic forces in the culture medium. To balance hydrodynamic forces against spheroid strength, it is necessary to assess the fluid dynamics in the STR.

We consider turbulent fluid dynamics within the STR. The most used mathematical description of turbulence was obtained by Kolmogorov. Kolmogorov´s model of isotropic turbulence can be used to describe the energy levels at different length scales as a cascade of eddies (**Figure 1 A**). If the eddy size is similar in magnitude to the spheroid size, then it is relevant for the hydrodynamic forces acting on the spheroids. The eddy cascade can be divided into macroscale and microscale components. On the macroscale, the mechanical power input of the stirrer leads to the formation of the initial anisotropic eddies (Λ_0). These have the highest kinetic energy, and their size is strongly influenced by the design of the stirrer. For a Rushton turbine, Λ_0 correlates to half of the stirrer height, h_S [6]. The anisotropic eddies decay into smaller eddies until they reach the microscale, on which eddies are no longer influenced by the stirrer's geometry and become isotropic. The microscale is divided further into the inertial and dissipation ranges. The viscosity of the culture medium is not relevant within the inertial range, but it becomes important within the dissipation range. Here, frictional resistance in the culture medium leads to the conversion of kinetic energy from the laminar flowing eddies into heat, which is known as energy dissipation. The energy dissipation ε correlates well with the kinetic energy of a certain eddy size [6]. The smallest existing eddy λ (Kolmogorov length) can be calculated, using the kinematic viscosity ν_L of the culture medium and mean energy dissipation $\bar{\varepsilon}$, as shown in Equation (1):

$$\lambda = \left(\frac{\nu_L^3}{\varepsilon}\right)^{\frac{1}{4}} \quad (1)$$

where

$$\varepsilon \propto \bar{\varepsilon} = \frac{P}{m} = \frac{N_P \cdot n^3 \cdot d_S^5}{V_L} \quad (2)$$

The energy dissipation in a STR is heterogeneous, but because the local energy dissipation is usually unknown, the mean energy dissipation $\bar{\varepsilon}$ is used instead. Equation (2) incorporates the stirrer-specific power number N_P, the stirrer frequency n, the diameter d_S, and the working volume V_L to determine $\bar{\varepsilon}$. The section, in which a spheroid of diameter d_{Sph} is stressed, can be estimated by λ. The relationship to discriminate the inertial and the dissipation ranges [1] is shown in Equations (3) and (4):

$$\text{Inertial range: } 25 \times \lambda < d_{Sph} < 0.1\,\Lambda_0 \quad (3)$$

$$\text{Dissipation range: } d_{Sph} < 6 \times \lambda \quad (4)$$

Whereas spheroids are transported along the streamlines of eddies that are much larger than the spheroid size, eddies that are similar in size to the spheroid diameter d_{Sph} are relevant to balance the hydrodynamic forces against the spheroid strength. Depending on the ratio of d_{Sph}/λ, either tensile or shear forces may dominate the stress acting on the spheroids.

At ratios of $d_{Sph}/\lambda > 3$, tensile forces become prevalent [7]. Spheroids exposed to tensile stress (**Figure 1 B**) by the culture medium, break into smaller agglomerates until an equilibrium between tensile forces and spheroid strength is reached [7,8]. The steady-state diameter can be assessed by balancing the hydrodynamic tension σ_T, and the adhesion force F_{ad} between the cells. The value of σ_T [7,9] can be calculated using Equation (5):

$$\sigma_T = (1 - P_F) \cdot \frac{F_{ad}}{d_{cell}^2} \quad (5)$$

where P_F is the porosity of the spheroid, and k is an empirical exponent, which describes the nature of the cell connection as shown in Equation (6):

$$(1 - P_F) = \left(\frac{d_{cell}}{d_{Sph}}\right)^k \quad (6)$$

At ratios of $d_{Sph}/\lambda < 3$, the spheroids are stressed by surface erosion due to laminar shear stress [7]. The shear stress σ_S (**Figure 1 C**), acting on the spheroid surface, can be estimated by calculating the pseudo-surface tension δ_{Sph}, which expresses the energy needed to form further cell connections [7], as shown in Equation (7):

$$\sigma_S = \frac{\delta_{Sph}}{d_{Sph}} \quad (7)$$

where the pseudo-surface tension δ_{Sph} can be expressed as shown in Equation (8):

$$\delta_{Sph} = (1 - P_F) \cdot \frac{F_{ad}}{d_{cell}} \quad (8)$$

The homogenous exposure of spheroids to hydrodynamic forces ensures a narrow size distribution, but this requires the development of a fully-turbulent regime. This criterion is fulfilled when a completely baffled STR [10] is processed at a Reynolds numbers (Re) of 5,000–10,000 [1]. The stirrer speed must be high enough to reach turbulence, but must remain within a range, in which the energy dissipation leads to the formation of spheroids in a desired size range. Both criteria are met at an energy dissipation of ~0.01 W kg^{-1}, leading to the predominant case of $d_{Sph}/\lambda < 3$, where a further consideration of tensile stress is unnecessary.

If one follows the cells through Kolmogorov's eddy cascade after seeding (**Figure 1 D**), the cells are initially transported convectively along the streamlines of the first eddies, until they reach the laminar eddies of the dissipation range. Cell collisions lead to small

agglomerates, which grow bigger, until the spheroids reach a certain size, at which the kinetic energy of eddies becomes too high, and further cell adhesion to the spheroids is prevented by surface erosion. Accordingly, the potential surface energy of the spheroids (or bonding energy E_{Bond}), and the kinetic energy of the eddies E_{kin}, must equalize to produce spheroids with a defined size, as shown in Equation (9):

$$\frac{E_{kin}}{E_{Bond}} = 1 \tag{9}$$

The kinetic energy is based on the momentum of the fluid [6], which can be defined as shown in Equation (10):

$$E_{kin} = \frac{\pi}{4} \cdot \rho_L \cdot \sqrt{u^2} \cdot d_{Sph}^3 = \frac{\pi}{4} \cdot \tau \cdot d_{Sph}^3 \tag{10}$$

with the fluctuation velocity u in the dissipation range [1] as shown in Equation (11):

$$\sqrt{u^2} = 0.0676 \cdot d_{Sph}^2 \cdot \frac{\bar{\varepsilon}}{\nu_L} \tag{11}$$

Furthermore, u and the fluid density ϱL can be used to determine the acting shear stress τ [1] as shown in Equation (12):

$$\tau = \rho_L \cdot \sqrt{u^2} \tag{12}$$

The bonding energy E_{Bond} is equal to the shear forces from Equation (7), acting on the surface of the spheroid as shown in Equation (13):

$$E_{Bond} = \delta_{Sph} \cdot \pi \cdot d_{Sph}^2 = (1 - P_F) \cdot \frac{F_{ad}}{d_{cell}} \cdot \pi \cdot d_{Sph}^2 \tag{13}$$

The adhesion force F_{ad} between the cells must be verified empirically, and depends on multiple factors such as the cell type, the culture medium, and the type of serum, if present, and the pre-culture harvest method. Nonetheless, the spheroid diameter d_{Sph} can be expressed as shown in Equation (14):

$$d_{Sph} = \frac{4 \cdot \delta_{Sph}}{\tau} \tag{14}$$

Increasing shear stress due to higher energy dissipation reduces the spheroid diameter d_{Sph}. This phenomenon is also observed for other model particles such as clay, latex, and glass [7–9,11–13].

The major adjustment screw, when manufacturing β-cell spheroids of a defined size, is therefore the energy dissipation, which is directly related to the stirrer type, and the resulting bioreactor setup. Not only is d_{Sph} determined by the power input, but the ratio $\varepsilon_{max}/\bar{\varepsilon}$ is crucial to achieve a spheroid formation with a narrow size distribution. The maximum energy dissipation ε_{max} can be found in regions close to the stirrer (the stirrer swept volume V_S), whereas the local energy dissipation ε_{loc} in regions far from the stirrer can be 10-fold lower. The aim is to minimize the $\varepsilon_{max}/\bar{\varepsilon}$ ratio by using a STR configuration with a comparable large stirrer to increase the stirrer-swept volume V_S in relation to the working volume V_L, and therefore a high stirrer diameter to tank diameter ratio ($d_S/D_T \geq 0.4$). The so-called bottom clearance C is the ratio of the stirrer diameter d_S to the installation height from the bottom $h_{S,Bottom}$, and values of $C \approx 0.2$ favor the production process [14]. The installation of sufficient baffling is essential.

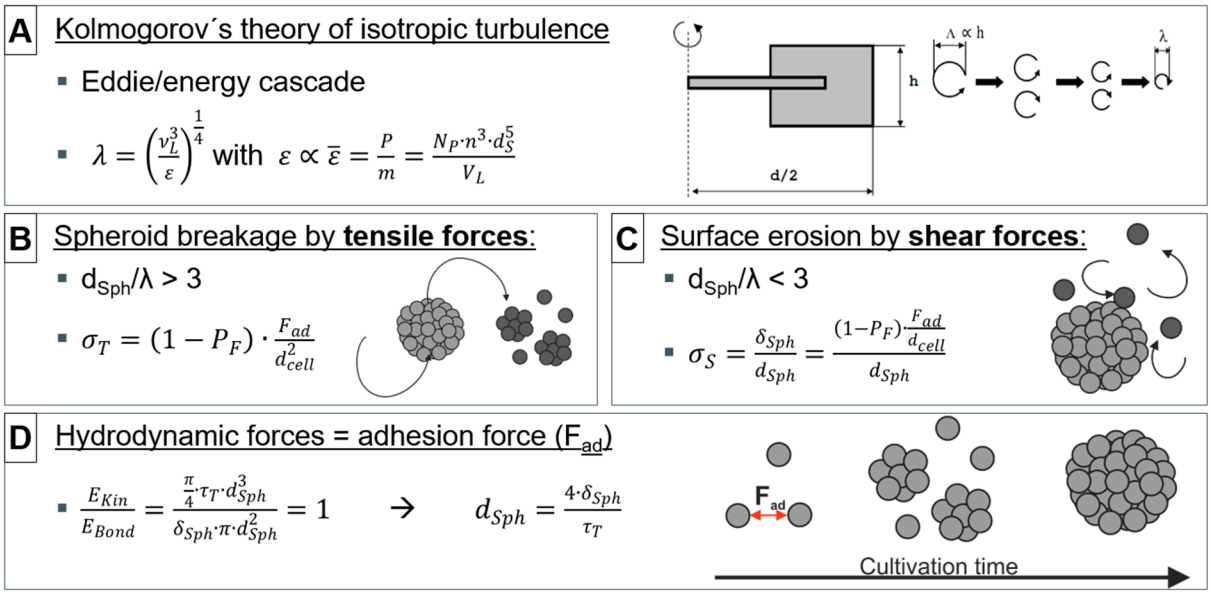

Figure S1. Schematic description of (A): the mechanical power input of the stirrer, the resulting eddy cascade and energy dissipation, followed by the two spheroid stress concepts involving (B) tensile forces, (C) surface erosion, and finally (D) spheroid agglomeration, until the hydrodynamic forces are in balance with the adhesion force Fad.

References

1. Henzler, H.J. Particle stress in bioreactors. *Adv. Biochem. Eng. Biotechnol.* **2000**, *67*, 35–82, doi:10.1007/3-540-47865-5_2.
2. Petry, F.; Weidner, T.; Czermak, P.; Salzig, D. Three-Dimensional Bioreactor Technologies for the Cocultivation of Human Mesenchymal Stem/Stromal Cells and Beta Cells. *Stem Cells Int.* **2018**, *2018*, 2547098, doi:10.1155/2018/2547098.
3. Hewitt, C.J.; Lee, K.; Nienow, A.W.; Thomas, R.J.; Smith, M.; Thomas, C.R. Expansion of human mesenchymal stem cells on microcarriers. *Biotechnol. Lett.* **2011**, *33*, 2325–2335, doi:10.1007/s10529-011-0695-4.
4. Pattappa, G.; Heywood, H.K.; Bruijn, J.D. de; Lee, D.A. The metabolism of human mesenchymal stem cells during proliferation and differentiation. *J. Cell. Physiol.* **2011**, *226*, 2562–2570, doi:10.1002/jcp.22605.
5. Langer, G.; Deppe, A. Zum Verständnis der hydrodynamischen Beanspruchung von Partikeln in turbulenten Rührerströmungen. *Chem.-Ing.-Tech.* **2000**, *72*, 31–41, doi:10.1002/1522-2640(200001)72:1/2<31:aid-cite31>3.0.co;2-o.
6. Wollny, S. Experimentelle und numerische Untersuchungen zur Partikelbeanspruchung in gerührten (Bio-)Reaktoren. Doctoral Thesis; Technische Universität Berlin, Berlin, 2010.
7. Mühle, K.; Domasch, K. Stability of particle aggregates in flocculation with polymers. *Chem. Eng. and Process.: Process Intensif.* **1991**, *29*, 1–8, doi:10.1016/0255-2701(91)87001-J.
8. Jarvis, P.; Jefferson, B.; Gregory, J.; Parsons, S.A. A review of floc strength and breakage. *Water Res.* **2005**, *39*, 3121–3137, doi:10.1016/j.watres.2005.05.022.
9. Schubert, H.; Mühle, K. The role of turbulence in unit operations of particle technology. *Advanced Powder Technology* **1991**, *2*, 295–306, doi:10.1016/S0921-8831(08)60696-2.
10. Heyter, A.; Wollny, S. Einfluss verschiedener Stromstörerausführungen auf die Bewehrung eines mehrstufigen Rührbehälters. *Chemie Ingenieur Technik* **2017**, *89*, 416–423, doi:10.1002/cite.201600188.
11. Kobayashi, M.; Adachi, Y.; OOI, S. Effect of Particle Size on Breakup of Flocs in a Turbulent Flow. *Proc. of Hydraul. Eng.* **2001**, *45*, 1249–1253, doi:10.2208/prohe.45.1249.
12. Oyegbile, B.; Ay, P.; Narra, S. Flocculation kinetics and hydrodynamic interactions in natural and engineered flow systems: A review. *Environ. Eng. Res.* **2016**, *21*, 1–14, doi:10.4491/eer.2015.086.
13. Wengeler, R.; Nirschl, H. Turbulent hydrodynamic stress induced dispersion and fragmentation of nanoscale agglomerates. *J. Colloid Interface Sci.* **2007**, *306*, 262–273, doi:10.1016/j.jcis.2006.10.065.
14. Kraume, M. *Mischen und Rühren: Grundlagen und moderne Verfahren;* Wiley-VCH: Weinheim, Germany 2003; ISBN 3527307095.